AIAA-2001-2407

PERFORMANCE ANALYSIS OF A WING WITH MULTIPLE WINGLETS

M. J. Smith[•], N. Komerath[+], R. Ames[↑], O. Wong[↑],
School of Aerospace Engineering, Georgia Institute of Technology, Atlanta, Georgia
and
J. Pearson[**]
Star Technology and Research, Inc., Mount Pleasant, South Carolina

ABSTRACT

This effort examined the potential of multi-winglets for the reduction of induced drag without increasing the span of aircraft wings. Wind tunnel models were constructed using a NACA 0012 airfoil section for the untwisted, rectangular wing and flat plates for the winglets. Testing of the configurations occurred over a range of Reynolds numbers from 161,000 to 300,000. Wind tunnel balances provided lift and drag measurements, and laser flow visualization obtained wingtip vortex information. The $Cobalt_{60}$ unstructured solver generated flow simulations of the experimental configuration via solution of the Euler equations of motion. The results show that certain multi-winglet configurations reduced the wing induced drag and improved L/D by 15-30% compared with the baseline 0012 wing. A substantial increase in lift curve slope occurs with dihedral spread of winglets set at zero incidence relative to the wing. Dihedral spread also distributes the tip vortex. These observations supplement previous results on drag reduction due to lift reorientation with twisted winglets set at negative incidence.

INTRODUCTION

In the 1970s, biologists began to look at the flying characteristics of soaring birds such as eagles, hawks, condors, vultures, and ospreys. Each of these birds has high lift wings with “pin” feathers at the ends that produce slotted wingtips. Biologists found that the pin feathers worked to reduce drag during gliding flight, as well as being used to provide roll control, in the same manner as ailerons on aircraft. These multi-winglets are quite often long and prominent, as in the case of the California Condor.

Modern interest in winglets spans the last 25 years. Richard Whitcomb of NASA Langley Research Center first looked at modern applications of winglets to transport aircraft in the 1970s. He used small, nearly vertical fins installed on a KC-135A and flight tested[1,2] in 1979 and 1980. The winglet concept actually dates back to a patent in 1897, but not until Whitcomb investigated winglet aerodynamics did the concept mature. Whitcomb showed that winglets could increase an aircraft's range by as much as seven percent at cruise speeds. A NASA contract[3] in the 1980s assessed winglets and other drag-reduction devices, and they found that wingtip devices (winglets, feathers, sails, etc.) can improve drag-due-to-lift efficiency by 10 to 15% if they are designed as an integral part of the wing. As add-on devices, however, they have been shown to be detrimental to overall performance of the wing.

Ilan Kroo et al[4] dealt with the broad concept of non-planar wings, which includes winglets. They reviewed a variety of aircraft types, including winglets, ring wings, box wings, and the exploitation of non-planar wakes in general. Such designs are of interest because of their potential for lower vortex drag without increased span, a key constraint for many aircraft. However, their effects on stability and control, characteristics of wake vortices, and structural implications of non-planar designs are also important.

The Wright brothers exploited the structural advantages of biplanes. At very low Reynolds numbers, highly cambered, thin sections perform better than thicker sections, making the cable-braced Wright biplane concepts especially

---

[•] Assistant Professor, Associate Fellow AIAA.
[+] Professor, Associate Fellow, AIAA.
[↑] Graduate Research Assistant, Student Member AIAA
[↑] Graduate Research Assistant, Student Member AIAA
** President, Associate Fellow AIAA

attractive. However, Gall and Smith[5] demonstrated that the addition of single winglets onto the biplanes added a 13% improvement in endurance, as well as increasing the lift-curve slope and the maximum lift coefficient of the vehicle.

In recent years, several types of wingtip improvements have been patented. The "spiroid" wing tip[6] produces a reduction in induced drag, much like that a winglet. Although a closed lifting system may eliminate the wing tips, it does not eliminate the trailing vortex wake.

Ruhlin, Bhatia, and Nagaraja[7] noted that the addition of a winglet substantially reduced the flutter speed of the wing at transonic Mach numbers. In addition, the effect of sideslip[8] on winglets is to produce increased loads analogous to wing loads caused by angle of attack. Satran[9] investigated the static and dynamic stability and control and free-flight behavior of a 0.36-scale model of a canard general-aviation airplane with a single pusher propeller and winglets in the Langley 30- by 60-Foot Wind Tunnel. He found the model to exhibit very stable dihedral effect but weak directional stability.

The blended winglet[10] reduces drag by eliminating the discontinuity between the wing tip and the winglet. A smoothed version is used on the gently upswept winglet of the Boeing 737-400. Boeing Business Jets and Aviation Partners, Inc. have embarked upon a cooperative program to market conventional winglets for retrofit to the Boeing 7xx series of jetliners. Flight tests on the Boeing Business Jet 737-400 resulted in a 7% drag reduction. Theoretical predictions had indicated that the configuration would have only a 1-2% improvement, and wind tunnel tests had shown only 2% drag reduction[11]. This indicates that wind tunnel test results of winglet configurations should be reviewed with some caution.

The first industry application of the winglet concept was in sailplanes. Colling[12] gives an excellent review of winglets for sailplanes that he investigated in the Texas A&M University 7x10 foot Low-Speed Wind Tunnel using a full-scale model of the outboard 5.6 feet of a 15-meter-class high performance sailplane wing. Marchman, Manor, and Faery[13] found that symmetric winglets were best for general aviation aircraft, but were less effective on tapered wings. Their tests also showed a reduction in wing wake turbulence from the winglets.

Robert Jones[14] described the advantages of single winglets for small transports, on which they can provide 10% reduction in induced drag compared with elliptical wings. Winglets are now being incorporated into most new transports, including the Gulfstream III and IV business jets[15], the Boeing 747-400 and McDonnell Douglas MD-11 airliners, and the McDonnell Douglas C-17 military transport.

Winglets can also be applied to hydrodynamic surfaces. Examples include the America's Cup sailboat keels with "winglets," as utilized by the 1983 America's Cup winner "Australia II."[16] The induced drag of a non-planar system can be lower than that of a planar system of the same lift and span. This is true even when the wing surfaces themselves are co-planar, but their vortex wakes are not. The keel and rudder (or twin keel surfaces) are coplanar, but due to the substantial leeway angle and longitudinal displacement of the two surfaces, the wake downstream of the boat resembles that of a biplane system, and the induced drag is reduced substantially.

Imamura[17] et al. analyzed the application of winglets to conventional wind turbines. They found that a small winglet installation angle causes a large increase in the power coefficient but a small increase in the flatwise bending moment compared with the blades with radially extended winglets. Rechenberg[18] describes a concentrator principle for wind turbines, which is used by birds with split wing ends. The wing tip vortices cause the flow to accelerate, which lowers the induced drag. He applied the concept to create a "wind lens" in which multiple high lift wings are arranged to form a circular fan about a wind turbine. The wind rotor in the center experienced a maximum power augmentation factor of more than 8.

There has been limited investigation of multiple winglets for aircraft. The split-tip design[19] by Heinz Klug for an aircraft wing can be considered a primitive multiple winglet. It was created to exploit the non-planar wake geometry by reducing induced drag and wing stress. Biologists have done extensive investigation of the split wingtips of soaring birds, which are found to be highly effective. Vance Tucker, a biologist with an aerodynamics background, demonstrated that the tip slots of soaring birds reduce induced drag and increase the span factor of the wings[20]. He found remarkable improvements of slotted wingtips compared with conventional wings with a Clark Y

airfoil. With the same increase in angle of attack, the Clark Y tip increased the base wing drag by 25%, while the feathered tip actually reduced the drag by 6%. In addition, the feathered tip maintained a high span factor under increasing angle of attack.

Work by evolutionary biologists at the Technical University of Berlin has also demonstrated the effectiveness of multiple slotted wings, and has shown how these features could have evolved naturally in birds through gradual increases in wing effectiveness. Their evolutionary theory has been emulated in an aircraft optimization algorithm developed by Kroo and Takai[21], which has "discovered" a C-wing configuration with a winglet and a horizontal extension that shows reduced drag for fixed lift, span, and height.

Jonathan Santos anticipated the innovation in the current proposal in his patent on wing-tip airfoils[22]. Santos recognized that a series of winglets at the wingtip could take advantage of the spiral nature of the wingtip vortices to improve the performance of a single winglet. Unfortunately, he allowed the patent to expire.

At the Cranfield Institute of Technology in England, J. J. Spillman carried out a series of programs to investigate devices akin to the wing tip airfoils, which he called "wing tip sails." He investigated the use of one to four sails on the wingtip fuel tank of a Paris MS 760 Trainer Aircraft[23]. Flight test experiments confirmed the wind tunnel tests, and demonstrated shorter takeoff rolls and reduced fuel consumption[24]. Spillman later investigated wingtip vortex reduction due to wing tip sails, and found lower vortex energy 400-700 m behind the aircraft, although the rate of decay beyond that was somewhat lower[25].

In Europe, an extension to the wing tip airfoils has been developed called Wing-Grid[26]. Wing-Grid is a set of multiple wing extensions added to the wing. These small wings are added at various angles so that their tip vortices do not interact to form a strong vortex. These smaller vortices dissipate the vortex energy so that the lift distribution is modified and the induced drag of the wing is reduced. This concept has been tested on a glider with good success. The concept is limited, since it is not able to change configuration in flight to optimize drag reduction. In addition, the closed latticework at the end of the wing does not allow the freedom to control the individual winglets for optimum configuration and performance. There may also be limitations due to aeroelastic effects in the compressible flight regime that have not yet been evaluated on the optimal configuration.

This effort examined the basic principles of multi-winglets. The multi-winglet design was evaluated to demonstrate its advanced performance potential over the baseline wing and an equivalent single winglet. A basic study of the flow-field physics surrounding the winglets and wing was performed with inexpensive models to guide selection of multi-winglet configurations. The number of winglets, their optimum shape, location and spacing, and their angles of attack, dihedral, and sweep were the unknowns to be determined.

EXPERIMENTAL CONFIGURATION

The experimental setup in the Georgia Tech 7' x 9' tunnel consists of a NACA 0012 semi-span wing with a 0.3 m (12") chord and a 1.219 m (48") span. Its root is mounted to a force balance located in the floor of the 2.13 m x 2.74 m (7' x 9') test section. The balance arm protrudes through the tunnel floor, so that the wing root is approximately 0.20 m above the floor. A short section of pipe and a disk (with a cutout) placed on top of the pipe are used to fair the balance and wing root. The 9mm clearance between the wing and the disk, needed to accommodate wing deflection due to balance deflection, was sealed using 5-mil plastic taped to both the wing and the disc. The plastic is used to create a known boundary condition, by preventing the pressure transmission between the suction and pressure sides of the wing.

The five winglets are flat aluminum plates with rounded leading edges, as shown in Figure 1. They have a span of 12in. and a chord of 1.5in. A mechanism in the wing tip allows for independent adjustment of the angle of attack and the rotation about the wing tip. Modeling clay was used to seal gaps between the wing tip and root of the winglet.

NUMERICAL CONFIGURATION

The computational portion of this research used the Cobalt$_{60}$[1] unstructured solver to generate flow simulations of the experimental configuration described in the previous section. Cobalt$_{60}$ solves the time-averaged Navier-Stokes equations, as well as the Euler subset of these equations. In conjunction with the wind tunnel experiments, three configurations have been chosen for numerical study:

- Baseline Wing (no winglets)

- Baseline Winglet Wing with 5 winglets located at tip with no dihedral
- Optimized Winglet Wing with 5 winglets located at 20^o, 10^o, 0^o, -10^o, -20^o dihedral from leading edge to the trailing edge

Computational grids for the unstructured $Cobalt_{60}$ code were developed, and a short grid optimization study on the baseline wing was performed. From this, a baseline grid was developed for application to the winglet configurations, and the numerical simulations with $Cobalt_{60}$ were performed. The control volume for the computations was set to be coincident to the wind tunnel walls so that computations could be directly compared with experimental data.

The baseline grid was modified by attaching five flat plate winglets along the z=0 line of the axisymmetric tip body. This models the configuration referred to in the experimental section as the baseline 0°, 0°,0°,0°,0° case. A sample orthogonal unstructured grid is given in Fig. 2.

RESULTS

Force Measurements

Various combinations of winglet dihedral (measured from the symmetry plane of the wing planform), as shown in Table 1, were evaluated in the GIT wind tunnel to determine the combination that provided the best improvement in lift-to-drag ratio (L/D). The Reynolds number was varied from 160,000 to 290,000, and force measurements for both untripped and tripped boundary layers were taken. As seen in Tables 2 and 3, which include a subset of these data, the best winglet dihedral configuration occurred when the winglets were equally separated by 10^o segments, decreasing from a 20^o dihedral for the leading edge winglet to a 20^o anhedral for the trailing edge winglet.

The increase from a 4ft span wing (Configuration 0) to the 5 ft span wing (Configuration 0a) is shown by an increase in the wing lift curve slope of about 2%. In contrast, the zero-spaced winglet (Configuration 1), produces an increase in lift curve slope of 10% for the higher speeds. There appears to be no dependence on whether the wing has been tripped or the boundary layer is permitted to transition naturally.

Further modification of the winglet dihedrals to different locations (Configurations 2 - 4 are presented) shows that the dihedral spacing of the winglets plays a major role in the lift curve slope values. Configuation 2 provided the largest increase of lift curve slope, ranging from 15% to 22% increases.

Further study was made of the performance of the wing. At chord Reynolds number of 290,000, the winglet effect on lift and drag can be seen in Figure 3. The tests were run in three configurations: winglets off (Configuration 0), winglets installed but all at zero degrees (Configuration 1), and winglets deployed at +20°, +10°, 0°, -10°, -20° (Configuration 3). Computational results from $Cobalt_{60}$ solving the Euler equations are also shown for Configurations 0 and 2. Note that in the calculation of C_L and C_D the reference area was 4 ft^2 for the winglets-off case and 5 ft^2 for both of the winglets-on cases. All experimental data were taken with a trip strip placed at approximately 5% chord on upper and lower surfaces. While the lift curve slope increases with the addition of the winglets (Fig. 3a), the drag increases (Fig. 3b), yielding an effective L/D for the winglets which is sometimes slightly lower than the L/D for the baseline wing (Fig. 3c). Similar results in the increase in lift curve slope (15% increase) were obtained by the numerical computations. At the lower speeds (and Reynolds numbers), some of the unexpected drag can be explained by the fact that induced drag may be dominating the zero-lift drag. As the speed is increased, the effects of the induced drag should diminish, as were observed in the experimental results. However, the L/D values measured even at the higher Reynolds number are still too low to be explained by induced drag.

This apparent anomaly can be explained by comparing with the results obtained by Spillman et al [23-25]. They showed that twisted winglets, set with the leading winglet at sharp negative incidence relative to the wing (geometric twist), improved L/D substantially (over 25%). The explanation was keyed to the nature of the upflow at the wing tip. The leading winglet is at moderate positive angle of attack with respect to the effective flow velocity at the wingtip, so that it produces lift. This lift vector, oriented perpendicular to the local velocity, thus has a substantial forward component, which cancels part of the drag, leading to a large improvement in L/D. The twist of their winglets accounts for the rapid decay of the upwash beyond the wing tip. Thus, in addition to dihedral, a negative geometric twist must be employed to ensure that the winglet is operating at optimal conditions.

This effect was verified by experiments at Ohio State University, in conjunction with this project, where winglet geometric twist was varied from winglets at the leading edge to the trailing edge. Winglet geometric twist was constant along the span of each winglet. As seen in Figure 4, the large negative dihedral at the leading winglets create a smaller induced drag. Lift coefficient for the overall wing is minimally affected by these geometric twist changes, thus the impact of geometric twist is felt in the drag. Full results of both studies can be found in Reference 27

The results plotted here are a small subset of the results obtained. The full data sets obtained via the Georgia Tech experiments can be found in Reference 28

Flow Visualization Results

A laser sheet was used to illuminate cross-sections of the flow downstream of the wing tip trailing edge, with smoke patterns videotaped from downstream. Images from two winglet / angle of attack settings are shown. The first set of images is from a run with the winglets set at dihedrals of +6, +3, 0, -3, -6 degrees respectively, the first value being the dihedral of the most upstream winglet. Here the angle of attack of both the wing and the winglets is 10 degrees. The images at lower angles of attack are similar but the vortices are not strong enough to show up clearly. The image from 5/12 chords downstream (Figure 5) shows one large vortex and at least two smaller ones rolling up around it. At 1 chord downstream there is one large vortex and one small one (Figure 6). At 2 chords (Figure 7) and 3 chords (not shown here) downstream, there is only one vortex. Thus the winglet vortices have merged into a single tip vortex, albeit one with larger core radius, by 2 chord lengths downstream of the trailing edge.

Figure 8 shows an image taken at 2 chords downstream in the test where the winglets were set at +20, +10, 0, -10, -20 degrees respectively. This is the setting previously determined to yield the best lift-to-drag ratio at the low Reynolds number of 161,000. The angle of attack is six degrees. For this configuration, five vortices are clearly visible in all of the downstream planes.

These experimental flow visualizations were compared to the numerical flow visualizations generated by $Cobalt_{60}$. Similar vortical flow very close to the wing was seen in the numerical results, but due to computer CPU limitations, the computational grids could not be adequately refined downstream in order to capture the fidelity of the vortex formation seen by the experimental results.

Presented in Figure 9 is an example of the change in vorticity magnitude at Mach 0.3 at the wingtip where it transitions to the spheroid endcap. These results are for an Euler simulation using $Cobalt_{60}$. The impact of the winglets (Configuration 1) is primarily the redistribution of the vorticity along the tip. The vorticity along the span of the winglets appear to be generating multiple, possibly counter-rotating vortices. The strength of these multiple, smaller vortices is substantially diminished from the baseline wing (Configuration 0) tip vortex. From classic Biot-Savart theory, it is recognized that there is a reduction of the overall downwash on the wing as these vortices exist farther from the main wing surface, and their individual strengths are diminished. In addition, for the optimized winglet configuration, the vortices appear to remain independent and do not seem to form one larger vortex, as seen in the baseline wing and winglet configurations. This multiple vortex configuration predicted by $Cobalt_{60}$ confirms the flow visualization of the experiments.

CONCLUSIONS

Experiments have been performed to examine the efficacy of multiple winglets mounted at varying dihedrals to improve the performance of a wng in subsonic flow. Combining the force measurement results with the flow visualization and the previous results of Spillman et al, the following 3 mechanisms are presented for performance improvement due to multiple winglets:

1. Negative incidence and twist of the winglets improves L/D by re-orienting the winglet lift vector forward and thus canceling part of the drag.
2. Flat plate winglets at zero incidence improve the lift curve slope, and produce more lift than an equivalent area of the baseline wing.
3. Dihedral spread of the winglets improves lift by taking some of the winglets away from the wing plane, and redistributing the tip vortex into multiple vortices that do not merge in the near wake, thereby reducing the effective downwash at the wing plane.

A combination of optimal dihedral and geometrically twisted winglets should provide enhanced L/D for subsonic wings over a range of Mach numbers.

ACKNOWLEDGMENTS

This research was sponsored by a SBIR Phase I study from the Air Force Research Laboratory, Wright-Patterson AFB, Ohio, Contract No. F33615-00-C-3017, Task 4 with Star Technology, Inc. The authors would like to thank the technical monitor, Mr. Chuck Jobe for his informative discussions with the authors, and Dr. Jerry Gregorek for permission to use Figure 4.

REFERENCES

1 Richard Whitcomb, "Methods for Reducing Aerodynamic Drag," NASA Conference Publication 2211, Proceedings of Dryden Symposium, Edwards, California, 16 September 1981

2 Richard Whitcomb, "A Design Approach and Selected Wind-Tunnel Results at High Subsonic Speeds for Wing-Tip Mounted Winglets," NASA TN D-8260, July 1976

3 Yates, John E., and Donaldson, Coleman duP., Fundamental Study Of Drag And An Assessment Of Conventional Drag-Due-To-Lift Reduction Devices, NASA Contract Rep 4004, Sep 1986

4 Ilan Kroo, John McMasters, and Stephen C. Smith, Highly Nonplanar Lifting Systems, Presented at: Transportation Beyond 2000: Technologies Needed for Engineering Design, NASA Langley Research Center, September 26-28, 1995

5 Gall, Peter D., and Smith, Hubert C., Aerodynamic Characteristics of Biplanes with Winglets, *Journal of Aircraft* v 24 n 8 Aug 1987 p 518-522

6 Louis B. Gratzer, Spiroid-Tipped Wing, U. S. Patent 5,102,068, 7 April 1992

7 Ruhlin, Charles L., Bhatia, Kumar G., and Nagaraja, K. S., Effects Of Winglet On Transonic Flutter Characteristics Of A Cantilevered Twin-Engine Transport Wing Model. NASA Technical Paper 2627 Dec 1986

8 Meyer, Robert R. Jr., and Covel, Peter F., Effects Of Winglets On A First-Generation Jet Transport Wing: VII—Sideslip Effects On Winglet Loads And Selected Wing Loads At Subsonic Speeds For A Full-Span Model. NASA Technical Paper 2619 Sep 1986 58p

9 Satran, Dale R., Wind-Tunnel Investigation Of The Flight Characteristics Of A Canard General-Aviation Airplane Configuration. NASA Technical Paper 2623 Oct 1986 59p

10 Reginald V. French, Vortex Reducing Wing Tip, U. S. Patent 4,108,403, 22 August 1978

11 Joe Clark, President, Aviation Partners, Inc., personal communication, 12 July 1999

12 Colling, James David, Sailplane Glide Performance And Control Using Fixed And Articulating Winglets. NASA-CR-198579 May 01, 1995

13 Marchman, J. F., III Manor, D., and Faery, H. F., Jr., Whitcomb Winglet Applications To General Aviation Aircraft, Aircraft Systems and Technology Conference Los Angeles, CA Aug. 21-23, 1978 AIAA Paper 78-1478

14 Jones, Robert T., Improving The Efficiency Of Smaller Transport Aircraft, 14th Congress of the International Council of the Aeronautical Sciences, Proceedings, Vol. 1, Toulouse, Fr, 1984

15 Chandrasekharan, Reuben M., Murphy, William R., Taverna, Frank P., and Boppe, Charles W., Computational Aerodynamic Design of the Gulfstream IV Wing. AIAA-85-0427, 1985

16 Slooff, J. W., On Wings And Keels (II). AIAA Monographs, v 31, p 67-85, Proceedings of the Fifteenth AIAA Symposium on the Aero/Hydronautics of Sailing, Seattle, September 21-22, 1985

17 Imamura, Hiroshi, Hasegawa, Yutaka, and Kikuyama, Koji, Numerical Analysis Of The Horizontal Axis Wind Turbine With Winglets, *JSME International Journal*, Series B v 41 n 1 Feb 1998 JSME Tokyo Japan p 170-176

18 Rechenberg, I., Vortex Screw, A New Concept For Wind Power Augmentation, European Wind Energy Conference 1984: Proceedings of an International Conference, Hamburg, Germany

19 Heinz G. Klug, Auxiliary Wing Tips for an Aircraft, U. S. Patent 4,722,499, 2 February 1988

20 Vance A. Tucker, Gliding Birds: Reduction Of Induced Drag By Wing Tip Slots Between The Primary Feathers, *Journal of Experimental Biology*, Vol. 180(1) 1993, pp. 285-310

21 Ilan Kroo and Masami Takai, A Quasi-Procedural, Knowledge-Based System for Aircraft Design, AIAA Paper AIAA-88-6502

22 Santos, Jonathan, Wingtip Airfoils, U. S. Patent 4,595,160, 17 June 1986

23 Spillman, J.J., "The use of wing tip sails to reduce vortex drag," *Aeronautical Journal*, Sep., 1978, pp. 387-395.

24 Spillman, J.J., Ratcliffe, H.Y., and McVitie, A., "Flight experiments to evaluate the effect of

wing-tip sails on fuel comsumption and handling characteristics," *Aeronautical Journal*, July, 1979, pp. 279-281.
25 Spillman, J.J., and Fell, M.J., "The effects of wing tip devices on (a) the performance of the Bae Jetstream (b) the far-field wake of a Paris Aircraft," Paper 31A, AGARD CP No. 342, Aerodynamics of Vortical Type Flows in Three Dimensions, Apr., 1983, pp. 31A-1-11.
26 La Roche, U., and Palffy, S., "WING-GRID, a Novel Device for Reduction of Induced Drag on Wings," Proceedings of ICAS 96, Sorrento, September 8-13, 1996
27 Pearson, J., Komerath, N., Smith, M. and Gregorek, J., "Multi-Winglets for the Reduction of Induced Drag," STAR, Inc. Report 2001-0201, Feb. 2001. Final Report for AFRL SBIR F33615-00-C-3017, Task 4.
28 GIT Experimental Group Website, http://www.adl.gatech.edu/archives.

Table 1. Multi-Winglet Combinations Experimentally Evaluated

Label	Configuration
0	Baseline 4 ft. span wing
0a	Baseline 5 ft. span wing
1	0^o, $0^{o,}$, 0^o, 0^o, 0^o
2	20^o, $10^{o,}$, 0^o, -10^o, -20^o
3	20^o, $20^{o,}$, 0^o, -20^o, -20^o
4	20^o, $20^{o,}$, 0^o, 20^o, 20^o
5	6^o, $3^{o,}$, 0^o, -3^o, -6^o
6	+10°, +5°, 0°, -5°, -10
7	+14°, +7°, 0°, -7°, -14°
8	+26°, +13°, 0°, -13°, -26°
9	+30°, +15°, 0°, -15°, -30°

Table 2: Lift curve slopes (per radian) for tripped wing (NM = not measured)

	0	0a	1	2	3	4
25 ft/s	3.84	NM	NM	4.38	NM	NM
65 ft/s	4.06	NM	4.49	4.65	NM	NM
85 ft/s	4.04	NM	4.62	4.70	NM	NM

Table 3: Lift curve slopes (per radian) for untripped wing

	0	0a	1	2	3	4
25 ft/s	3.99	4.07	4.11	4.89	3.94	4.00
65 ft/s	4.25	4.31	4.69	4.96	4.79	4.23
85 ft/s	NM	4.62	NM	NM	NM	NM

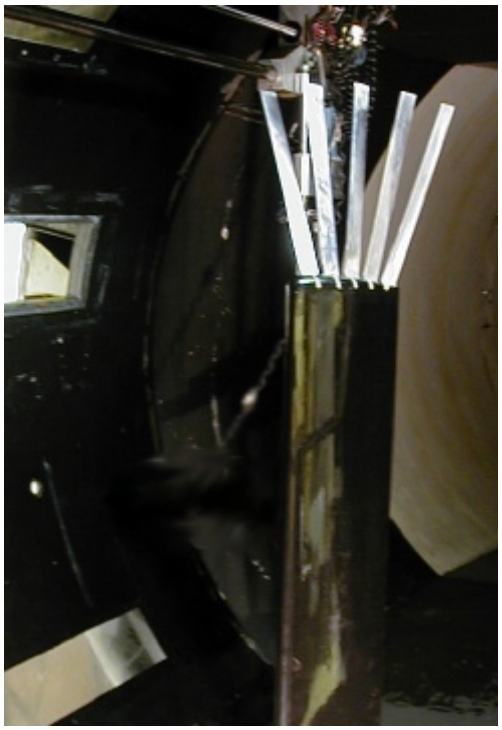

Figure 1. Wing model with winglets

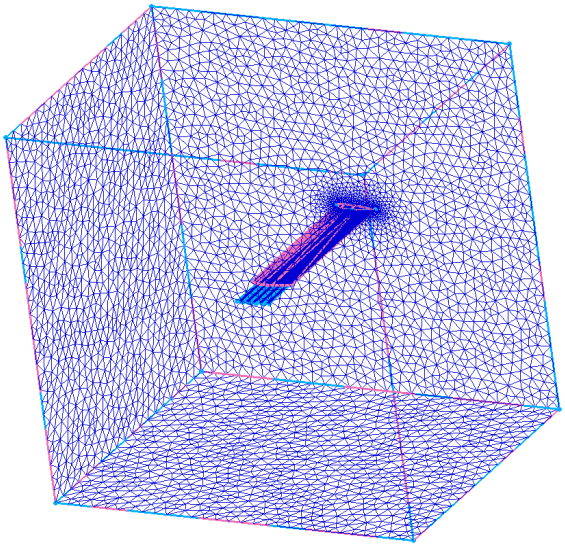

Figure 2. Sample Euler Grid for the Baseline Winglet Configuration

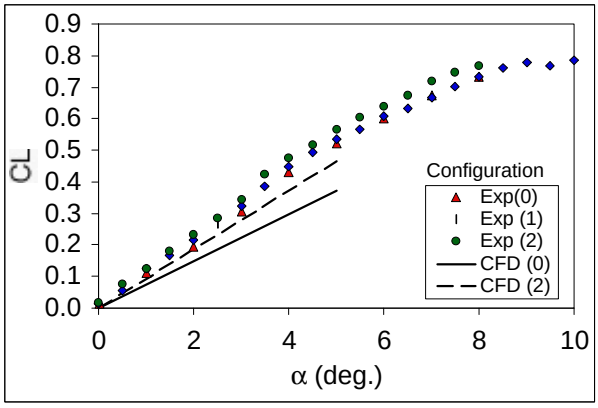

a) Effect on lift coefficient vs. angle of attack

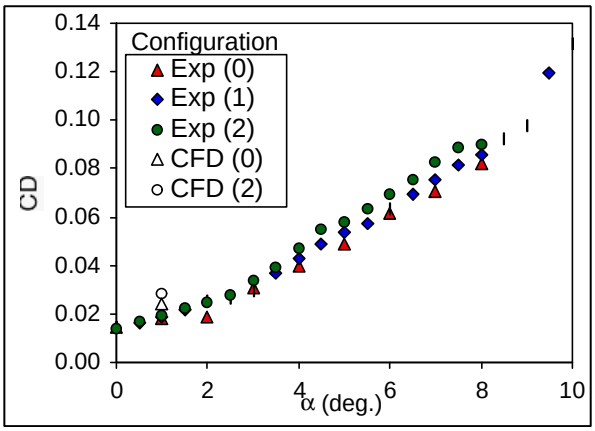

b) Effect on drag coefficient vs. angle of attack

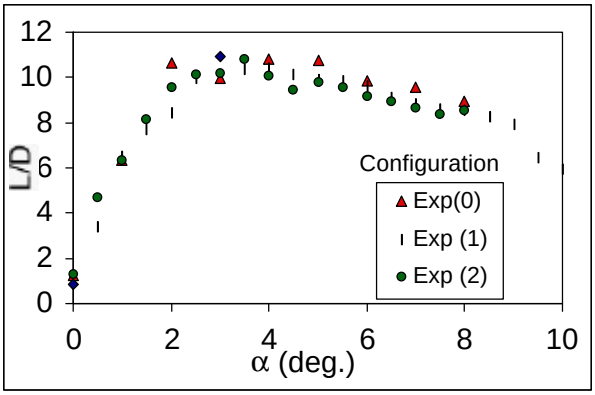

c) Effect on drag polar

Figure 3. Results for the NACA0012 wing at a chord Reynolds Number of 290,000

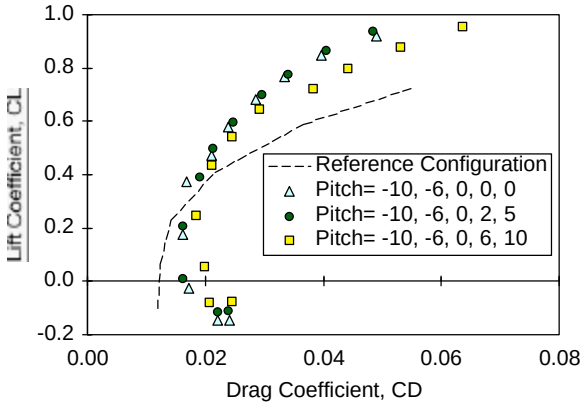

Figure 4. Results for the NACA0012 wing at a chord Reynolds Number of 600,000 for different winglet geometric twist variations. From Ref. 27

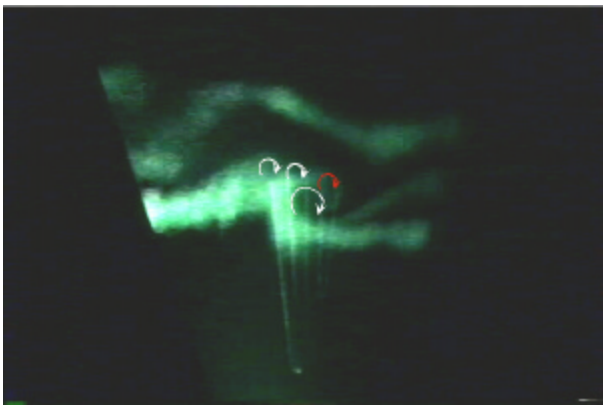

Figure 5. Laser sheet images from 5/12 chords downstream with winglets at dihedrals of +6, +3, 0, -3, -6 degrees

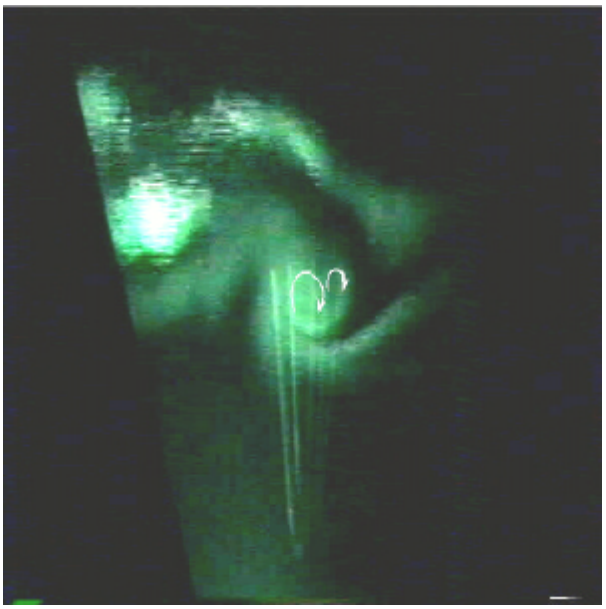

Figure 6. At 1 chord downstream, there is one large vortex and one small one

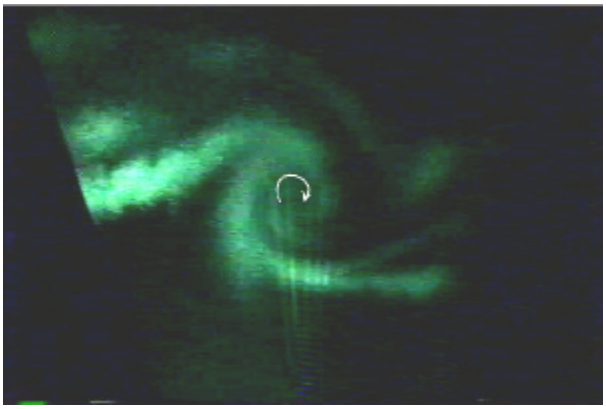

Figure 7. At 2 chords and 3 chords (not shown here) downstream, there is only one vortex

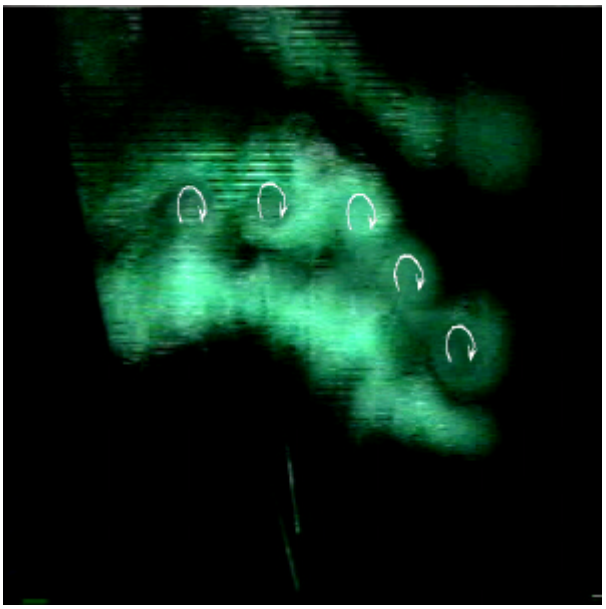

Figure 8. At 2 chords downstream with the winglets at best setting of +20, +10, 0, -10, -20 degrees respectively, which yielded the best L/D at Re of 161,000

Figure 9. Comparison of the numerically predicted vorticity over the main wing endcap. Top view shows baseline wing (Configuration 0), middle view the baseline winglet (Configuration 1), bottom view is the optimized dihedral wing (Configuration 2).